Mountain building and mantle dynamics

Claudio Faccenna,[1] Thorsten W. Becker,[2] Clinton P. Conrad,[3] and Laurent Husson[4,5]

Received 14 June 2012; revised 20 August 2012; accepted 6 December 2012; published 27 February 2013.

[1] Mountain building at convergent margins requires tectonic forces that can overcome frictional resistance along large-scale thrust faults and support the gravitational potential energy stored within the thickened crust of the orogen. A general, dynamic model for this process is still lacking. Here we propose that mountain belts can be classified between two end-members. First, those of "slab pull" type, where subduction is mainly confined to the upper mantle, and rollback trench motion lead to moderately thick crustal stacks, such as in the Mediterranean. Second, those of "slab suction" type, where whole-mantle convection cells ("conveyor belts") lead to the more extreme expressions of orogeny, such as the largely thickened crust and high plateaus of present-day Tibet and the Altiplano. For the slab suction type, deep mantle convection produces the unique conditions to drag plates toward each other, irrespective of their nature and other boundary conditions. We support this hypothesis by analyzing the orogenic, volcanic, and convective history associated with the Tertiary formation of the Andes after ~40 Ma and Himalayas after collision at ~55 Ma. Based on mantle circulation modeling and tectonic reconstructions, we surmise that the forces necessary to sustain slab-suction mountain building in those orogens derive, after transient slab ponding, from the mantle drag induced upon slab penetration into the lower mantle, and from an associated surge of mantle upwelling beneath Africa. This process started at ~65–55 Ma for Tibet-Himalaya, when the Tethyan slab penetrated into the lower mantle, and ~10 Myr later in the Andes, when the Nazca slab did. This surge of mantle convection drags plates against each other, generating the necessary compressional forces to create and sustain these two orogenic belts. If our model is correct, the available geological records of orogeny can be used to decipher time-dependent mantle convection, with implications for the supercontinental cycle.

Citation: Faccenna, C., T. W. Becker, C. P. Conrad, and L. Husson (2013), Mountain building and mantle dynamics, *Tectonics*, *32*, 80–93, doi:10.1029/2012TC003176.

1. Introduction

[2] Mountain belts show different styles and architectures [e.g., *Dewey and Bird*, 1970; *Royden*, 1993a]. Some orogens resemble crustal-scale accretionary prisms [*Platt*, 1986], created by piling up of crustal slices scraped from the downgoing plate. This type of mountain range, typical of the Mediterranean mobile belt, forms without large relative plate convergence under the pull of subducting oceanic and delaminating continental lithosphere [*Royden*, 1993b; *Jolivet et al.*, 2003; *Brun and Faccenna*, 2008]. Such mountains are characterized by low elevation, small crustal thickness, and the presence of extensional structures [*Royden*, 1993a; *Doglioni et al.*, 1999], dissecting their inner portion and exhuming deeper crustal layers [*Brun and Faccenna*, 2008]. The other orogenic type, on which we focus here, is made of thick crustal piles derived from both downgoing and upper plates that form, under extreme conditions, high-elevation plateaus such as in the Altiplano-Puna or Tibet, where the crust can be up to ~80 km thick [e.g., *Hatzfeld and Molnar*, 2010] (Figure 1). We suggest that these two orogenic types can be considered end-members of a continuous spectrum on Earth. The purpose of this contribution is to explore the dynamic conditions generating the extreme settings necessary to form thick-crustal orogens, presently expressed as the Central Andes Cordillera and the Tibetan-Himalayan belt.

[3] The Cordilleras formed by the subduction of the Farallon and Nazca plates beneath the Americas date back at least to the Paleozoic. The recent Andean belt of South America formed during the Tertiary; up to the Late Cretaceous, southern America was under extension. Only during the last ~50 Myr did compressional stresses increase, inverting extensional basins and creating a mountain belt [*Oncken et al.*, 2006]. The Andes are mostly made of slices

[1]Laboratory of Experimental Tectonics, Università degli Studi Roma Tre, Rome, Italy.
[2]Department of Earth Sciences, University of Southern California, Los Angeles, California, USA.
[3]Department of Geology and Geophysics, SOEST, University of Hawaii, Honolulu, Hawaii, USA.
[4]Géosciences Rennes, Université de Rennes 1, UMR 6118, CNRS, Rennes, France.
[5]Laboratoire de Planétologie et Géodynamique de Nantes, UMR 6112, CNRS, Nantes, France.

Corresponding author: C. Faccenna, Laboratory of Experimental Tectonics, Università degli Studi Roma Tre, Largo S. L. Murialdo 1, 00146 Rome, Italy. (faccenna@uniroma3.it)

0278-7407/13/2012TC003176

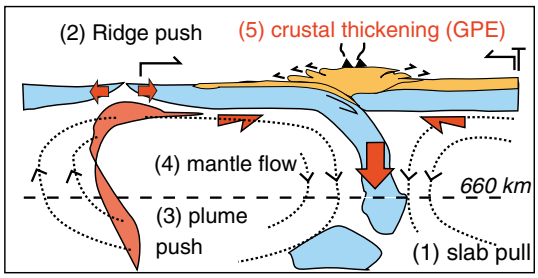

Figure 1. Cartoon illustrating major force components of mantle convection during mountain building at convergent margins.

of South American upper crust and by intrusion of igneous material, reaching a maximum crustal thickness of ~70 km in the Bolivian orocline [e.g., *Beck et al*., 1996]. From a kinematic point of view, shortening is related to the westward advancement of South America toward the stationary/slowly retreating Nazca trench. *Russo and Silver* [1996] and *Schellart et al*. [2007] suggested that the stationarity of the Nazca trench around the Bolivian orocline is related to the overpressure of subslab mantle in the center of the slab, preventing slab retreat. However, this model fails to explain why the Nazca subduction system rolled back during the opening of the Southern Atlantic for almost 100 Myr, and only at ~50 Ma decreased its retrograde motion [*Husson et al*., 2012].

[4] The Alpine-Himalayan belt formed on the site of subduction of the Tethyan Ocean, active at least from the Jurassic, accreting continental blocks against the Asian continent [*Dercourt et al*., 1986; *Pubellier et al*., 2008]. India separated from Gondwanaland at ~90 Ma and, after very fast drift between 67 and 52 Ma, decelerated, "indenting" and underthrusting Asia for ~1000 km [e.g., *Patriat and Achache*, 1984; *Rowley*, 1996; *Najman and Garzanti*, 2000; *van Hinsbergen et al*., 2011a]. The Tibetan plateau is the product of this impressive collision, where trench advance accommodated most of the plate velocity, such that the subduction velocity almost vanished.

[5] For Tibet, the origin of the forces that push India into Asia is still debated. The majority of models suggest that driving forces derive from the pull exerted by the downwelling of oceanic plates or by the delaminated mantle of the continental lithosphere (Figure 1) [*Copley et al*., 2010; *Capitanio et al*., 2010]. Slab pull is the dominant force for plate motions, but it counteracts collision because slab pull should promote retreating trenches and generally prevent the generation of large compressive stresses [*Molnar and Atwater*, 1979; *Garfunkel et al*., 1986]. The hinge of the subducting plate, even for the case of continental lithosphere, can retreat if the deep or surface load is high enough to overcome the bending resistance, as, for example, for the Apennines/Carpathian [*Royden et al*., 1987]. Moreover, in collisional zones such as India or Arabia, slab pull is expected to be reduced to its minimum level, given the inferred repeated episodes of slab break-off [e.g., *Chemenda et al*., 2000; *Faccenna et al*., 2006; *Hafkenscheid et al*., 2006; *Keskin*, 2003; *Replumaz et al*., 2010].

[6] Another important force is ridge push, due to the thermal thickening of the oceanic lithosphere. Estimates of ridge push for the Indian Ocean are ~10^{12} N/m, increasing by a factor of 3–4 for large oceanic plates such as the Atlantic [e.g., *Schubert et al*., 2001]. For the case of Tibet, ridge push may, however, be insufficient to sustain orogeny [*Ghosh et al*., 2006]. The third potential driving force is related to the arrival of mantle plumes at the base of the lithosphere. Thermal upwellings can lead to increased driving tractions and a reduction of asthenosphere viscosity, facilitating lithospheric motions [e.g., *van Hinsbergen et al*., 2011b]. This mechanism was first proposed to explain the rapid drift of continental plates, such as Laurentia or Baltica, when velocities are in excess of 10 cm/yr [*Gurnis and Torsvik*, 1994] and was then applied to the acceleration of India during the emplacement of the Deccan large igneous province (LIP) [*Cande and Stegman*, 2011; *van Hinsbergen et al*., 2011b]. However, the effect of a small-scale plume push is expected to be temporary, lasting only a few million years [*van Hinsbergen et al*., 2011b]. For the case of India, it may contribute to the observed peaked velocity and subsequent deceleration but cannot explain the protracted collisional velocity [*van Hinsbergen et al*., 2011b]. The fourth contribution is represented by the drag exerted by large-scale mantle flow, sometimes called "continental undertow" [*Doglioni et al*., 1999; *Alvarez*, 1990, 2010]. Mantle drag associated with upwellings and large-scale downwellings has been suggested as an efficient mechanism for propelling India in the present day [*Becker and Faccenna*, 2011] and rapid continental plate motions in general. However, the mantle drag amplitude will depend on the time-dependent vigor of mantle convection.

[7] For orogens to be created and sustained, the sum of the acting forces such as slab pull, ridge push, plume push and large-scale, mantle flow–related tractions must balance the resisting forces. Those are mainly represented by the gravitational potential energy (GPE) stored within the thick crustal column, the viscous dissipation in the deforming mantle and lithosphere, and the resisting forces necessary to slide along thrust/subduction faults (Figure 1). In particular, the lithospheric opposition to compressional stresses depends on a trade-off between GPE stored within an already-uplifted mountain belt and convergent deformation that generates this uplift. During the infant stage of mountain building, all the driving forces are balanced by convergent strain within the lithosphere, whereas during the late orogenic stage, most of the forces are expected to be balanced by the GPE stored within the mountain belt. The frictional sliding resistance will be important during the formation of crustal stacks and will depend on the details of the strain-localization mechanism and fault strength. The effect of the GPE in Tibet or the central Andes corresponds to forces of the order of ~8–9 · 10^{12} N/m [*Molnar et al*., 1993; *Ghosh et al*., 2006; *Husson and Ricard*, 2004].

[8] Previously, we investigated the role of slab pull, plate interactions, and mantle flow on the present-day motion of the South American plate [*Husson et al*., 2012] and the India-Arabia system [*Becker and Faccenna*, 2011]. These studies emphasized that mantle flow is an efficient mechanism to drag India, Arabia, and South America in the right directions. Here we extend the analysis to the possible far-field connections within the India-Africa-South America system, and the time dependence of mountain building throughout Earth's history.

[9] To test the mantle's role in building mountain belts by pulling or dragging plates, we performed a series of new global circulation models that compute mantle flow from density anomalies. We use these to first describe the

kinematics of the South America-Africa-India system and then to compare the mantle structure beneath the Andes and the Himalaya with the computed mantle flow, discussing the role of mantle drag, subducting slabs, and their combination in a globally coupled system. We then discuss the tectonic history of the belts and argue that they both have the same deep-rooted mantle origin, irrespective of their differences in plate structure and boundary conditions.

2. Kinematic Evolution of the Indo-Atlantic System

[10] Around 130 Ma, the South Atlantic Ocean started opening, with the separation of South America from Africa. The earlier breakup phases of east Gondwana date back to the Jurassic with the separation of Madagascar and Antarctica from Africa after the Karoo LIP emplacement [*Jourdan et al*., 2007; *Eagles and König*, 2008; *Gnos et al*., 1997]. This was followed by spreading between India and Antarctica and the Kerguelen LIP emplacement at ~130 Ma [*Gaina et al*., 2007]. Since the Late Cretaceous, the kinematics of the South America-Africa-India system show intriguing features [*Silver et al*., 1998; *Conrad and Lithgow-Bertelloni*, 2007; *Cande and Stegman*, 2011], summarized in Figure 2. Around 90 Ma, during the emplacement of the 91–84 Ma Morondava LIP, seafloor spreading localized between Madagascar and India/Seychelles [*Torsvik et al*., 2000; *Bardintzeff et al*., 2010]. Just after the emplacement of the Morondava LIP, India shows a temporary increase in velocity to ~11 cm/yr on average [*van Hinsbergen et al*., 2011b], returning back to ~8 cm/yr at ~83 Ma. Eventually, after the emplacement of the Deccan LIP by the Reunion plume at ~65.5 Ma, an eastward jump of the spreading ridge between India and Madagascar transferred the Seychelles microcontinent from the Indian plate to Africa (Figure 2a) [*Hofmann et al*., 2000; *Collier et al*., 2008]. During this phase, the velocity of India sharply sped up to 16–18 cm/yr (Figure 2e) [*Patriat and Achache*, 1984; *Copley et al*., 2010; *van Hinsbergen et al*., 2011b], with an increase of the Indian Ocean spreading rate of up to ~50% (Figure 2d) [*Conrad and Lithgow-Bertelloni*, 2007; *Cande and Stegman*, 2011]. During the Eocene (~55–50 Ma), India's speed progressively decreased to the present-day value of ~4–5 cm/yr (Figures 2b and 2d) [*Zhang et al*., 2004; *Copley et al*., 2010]. This deceleration has been commonly related to the collision of continental India with Asia at ~50 Ma [*Molnar and Tapponnier*, 1975; *Najman and Garzanti*, 2000; *Guillot et al*., 2003; *Hatzfeld and Molnar*, 2010].

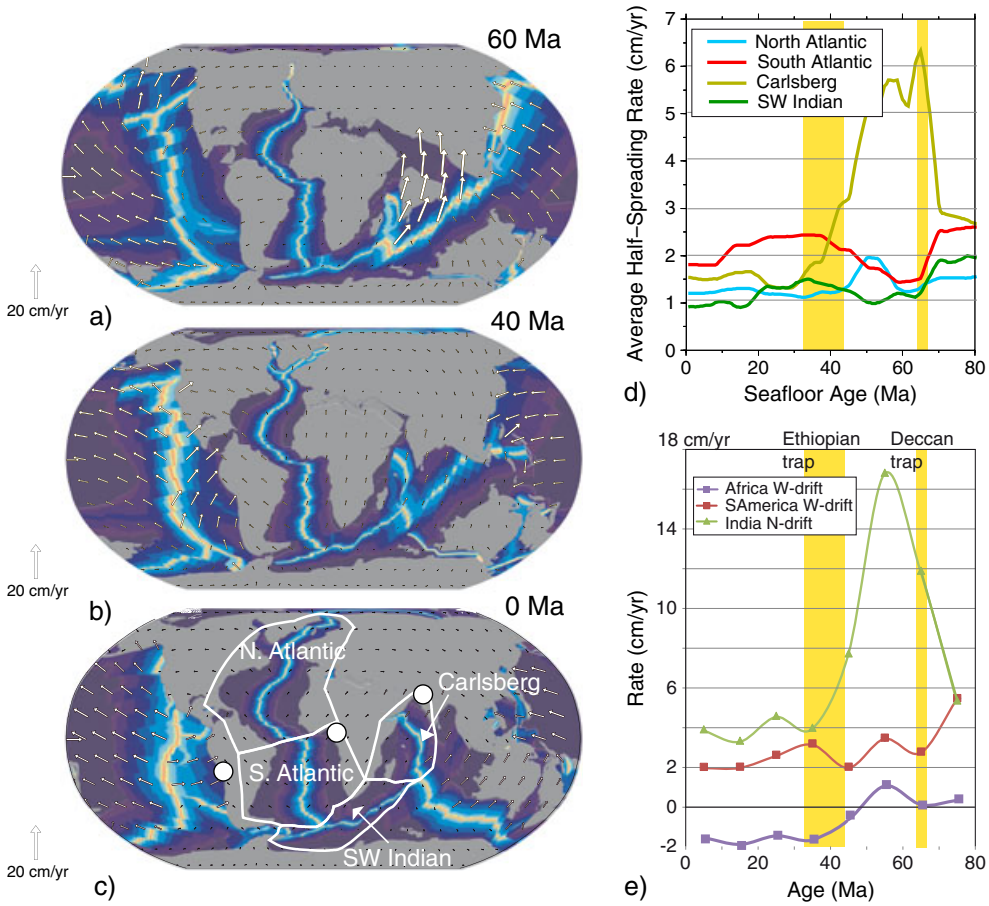

Figure 2. Three-stage evolution of plates velocity at (a) 60 Ma, (b) 40 Ma, and (c) the present day from GPlates (*Müller et al*. [2008] velocity model). (d) Half-spreading rate of South Atlantic, North Atlantic, Carlsberg, and South Indian Ocean basin ridge systems (see domains on Figure 2c) from *Conrad and Lithgow-Bertelloni* [2007]. (e) Velocity of one point (location on Figure 2c) giving the westward component of motion of South America and Africa and the northward motion of India from *Müller et al*. [2008]. Yellow strips in Figures 2d and 2e mark the age of emplacement of Deccan and Afar traps.

[11] During the rapid Tertiary drift of India, Africa and South America also show related changes in plate motion. This linkage is well illustrated by the anticorrelation in the spreading rate between the South Atlantic and Indian Ocean (Figure 2d) [*Conrad and Lithgow-Bertelloni*, 2007]. Recent reconstructions show that, while India was moving rapidly northward (~65–55 Ma), Africa's motion changed from a NNE toward a NNW direction [*Dewey et al*., 1989; *Müller et al*., 2008; *Torsvik et al*., 2010; *Cande and Stegman*, 2011]. As South America did not show any significant change in motion, this alteration in African motion resulted in a decrease of the South Atlantic spreading rate (Figures 2d and 2e) [*Conrad and Lithgow-Bertelloni*, 2007]. After, from ~45 to ~25 Ma, the modest increases in the rate of South American westward drift and the change to a NNE-directed motion of Africa produced an increase of the South Atlantic spreading rate, rising back to ~4 cm/yr [*Conrad and Lithgow-Bertelloni*, 2007].

[12] These kinematic linkages between the motions of India, Africa, and South America support the concept of an intrinsic connection between the deep mantle and the lithosphere of the plates that form the Indo-Atlantic "box" circuit [*Silver et al*., 1998; *Davaille et al*., 2005].

3. Present-Day Mantle Structure and Flow Beneath Mountain Belts

[13] Orogens have long been related to the deep mantle: the "circum-Pacific and Alpine-Himalayan mountain systems are due to compression over downward flowing limbs of huge convection cells" [*Wilson*, 1961]. Global mantle tomography now illuminates the structure of the mantle beneath the orogens and allows us to make quantitative assessments. We will mainly discuss patterns of flow associated with the composite tomography model SMEAN [*Becker and Boschi*, 2002], because it has been found to yield good matches to

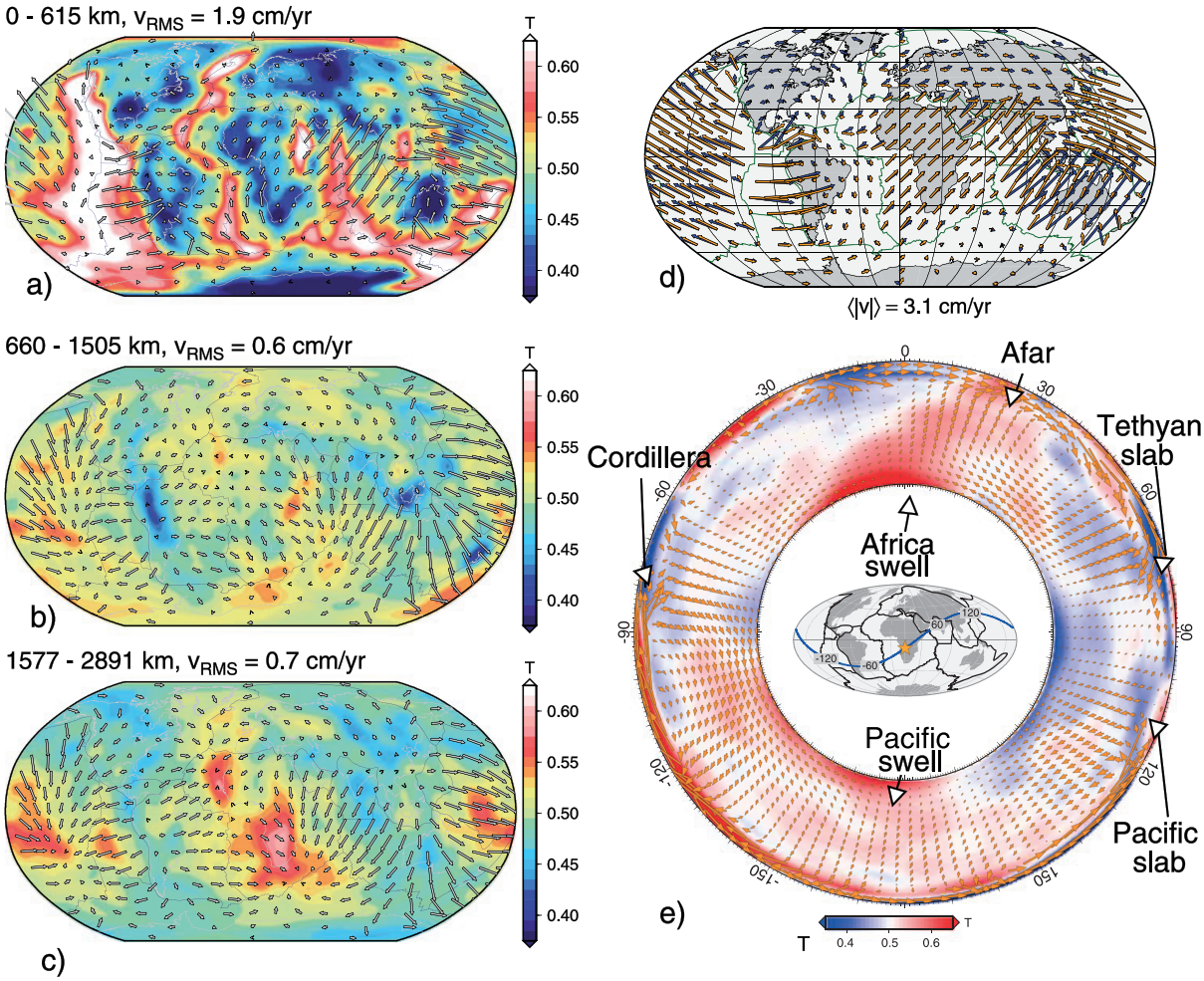

Figure 3. Reference mantle flow solutions as inferred from SMEAN composite tomography and viscous tomography inversion [cf. *Ghosh et al*., 2010; *Becker and Faccenna*, 2011] averaged over three different depth ranges: (a) 0–615 km, (b) 660–1505 km, and (c) 1577–2891 km. (d) Cross section (location shown in central inset) showing the presence of two large upwelling and downwelling zones forming four large-scale convection cells. The Andes and the Himalaya are located on top of, and are inferred to be sustained by, deep mantle downwellings. (e) Comparison between NUVEL-1A model (blue arrows) [*DeMets et al*., 1994] and expected plate velocity from mantle flow (red arrow). Linear correlation coefficient is 0.93, computed as in *Ghosh et al*. [2010]. All velocities shown are in the no-net-rotation reference frame.

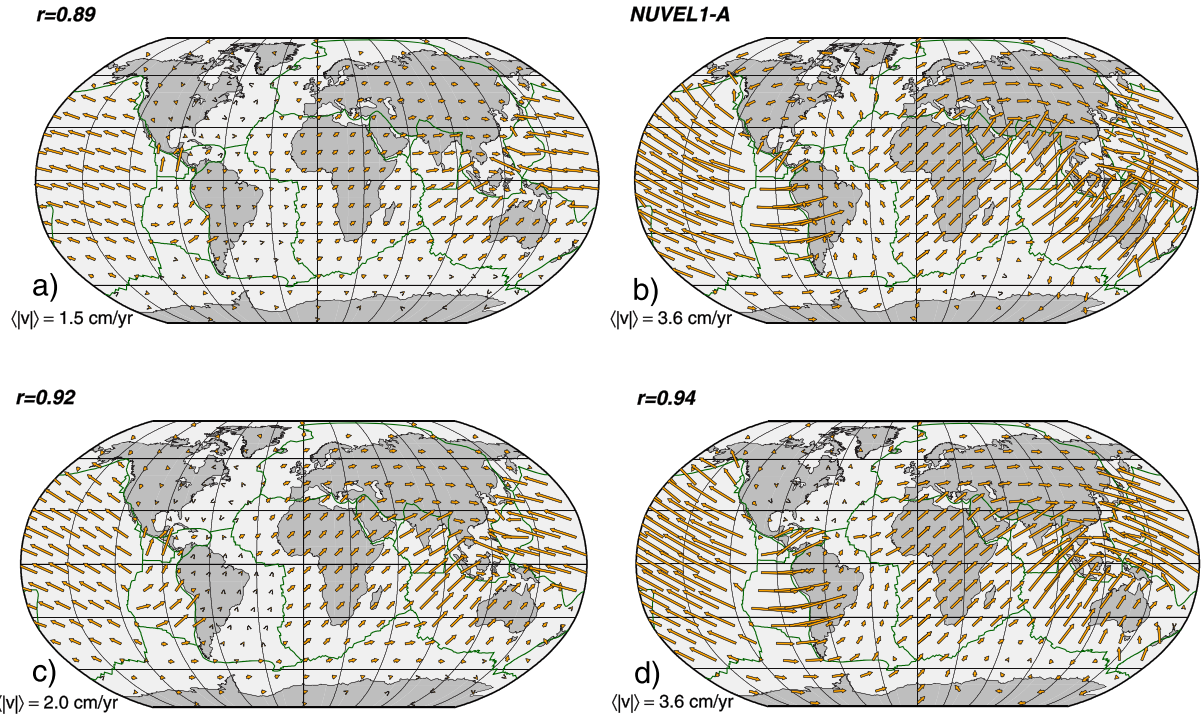

Figure 4. Additional flow solutions for global plate motions for different density models. Surface velocities are the same as on Figure 3e. (a) Flow generated by upper mantle slab density anomalies restricted to Wadati-Benioff zones. (b) Plate motions for the NUVEL-1A model. (c) Flow generated by upper mantle slabs and lower mantle density anomalies as inferred from tomography as in the reference model of Figure 3. (d) Flow generated as in Figure 4c but also including "hot" upper mantle anomalies from tomography (using slow velocity anomalies only; cf. *Becker and Faccenna* [2011]).

constraints such as the geoid [*Steinberger and Calderwood*, 2006] or surface wave arrival times [*Qin et al.*, 2009], but use of other, including more recent, global tomographic models would lead to very similar conclusions.

[14] The two main orogenic belts, the Andean Cordillera and the Alpine-Himalaya, are indeed located over two prominent, positive velocity anomalies (inferred to be cold and hence sinking; Figures 3 and 4). The first one extends roughly N-S from the Great Lakes to Patagonia and is well delineated at the bottom of the upper mantle and in the lower mantle (Figures 3b and 4) [*Grand et al.*, 1997; *Bunge et al.*, 1998; *Ren et al.*, 2007]. The other anomaly extends from the eastern Mediterranean to Indonesia [*van der Voo et al.*, 1999; *Replumaz et al.*, 2004]. It is broken into smaller portions along the suture zone of the Bitlis-Zagros-Himalayan belt (Figures 3a and 4) but gets continuous and more pronounced ($\delta V_S = \mathrm{d}V_S/V_S = \mathrm{d}\ln V_S \geq 1\%$) at greater depth (Figures 3b and 4). At its eastern end it merges with the western Pacific, which corresponds to a well-defined but discontinuous belt in the upper mantle (Figure 3a), with a localized middle mantle signature beneath the Izu-Bonin [*van der Hilst and Seno*, 1993] (Figure 4) and almost no penetration to deeper levels.

[15] Those two lower mantle, high-velocity anomalies positioned beneath the Andean Cordillera and the Alpine-Himalaya surround the large, low-shear-wave-velocity province (LLSVP) [e.g., *Garnero and McNamara*, 2008] beneath Africa (Figure 3) [*Su and Dziewonski*, 1997; *Ritsema et al.*, 1999; *Davaille et al.*, 2005]. This LLSVP is likely related to a thermal and, particularly at larger depths, partially chemical anomaly [e.g., *Ni et al.*, 2002; *McNamara and Zhong*, 2005]. In the upper mantle the low-velocity zone is restricted to the Afar region and to the northeastern Indian ridge (Figure 3a), extending in the transition zone to the east of Madagascar and beneath Tibesti (Figures 3a and 3b). In the shallow lower mantle the low-velocity anomaly extends to parts of West Africa and near the East African rift zone. At 1500–2000 km depth, low velocities are more pronounced ($\delta V_S \leq -1\%$), extending over most of South Africa in a N-S direction, separated from a West Africa low-velocity anomaly [*Davaille et al.*, 2005] (Figure 3c). At the base of the lower mantle, Africa would be almost entirely covered by the LLSVSP. Large igneous provinces at the surface are found around this low-velocity zone [*Burke and Torsvik*, 2004], suggesting a causative link of extended duration beneath the core of Africa [*Torsvik et al.*, 2008].

[16] Here we use global mantle flow computations to test the influence of different models for mantle density heterogeneity and/or the subducting lithosphere on present-day plate motion. We compute the instantaneous mantle flow driven by density heterogeneity inferred from seismic tomography when velocity anomalies are converted into temperature [e.g., *Hager and Clayton*, 1989; *Lithgow-Bertelloni and Silver*, 1998; *Gurnis et al.*, 2000]. We solve the Stokes equation for incompressible flow in a global, spherical shell using a finite-element approach [*Zhong et al.*, 2000]. The

basic model setup is discussed in *Becker and Faccenna* [2011], but here we use results of a guided optimization (described below) that treats geologically motivated lateral viscosity variations as adjustable parameters and leaves the assumed mantle density distributions as simple as possible. This optimizes the global fit to plate motions and is done to show that entirely force-consistent plate motion models can result from simple velocity-density scaling assumptions for the mantle. However, the broad patterns of mantle-rooted driving forces in our models are mainly controlled by the assumed density structure, and our general conclusions are independent of this optimization.

[17] The reference density structure is based on SMEAN, with fast continental keel structures above 300 km removed to correct for shallow compositional effects. We use a Rayleigh number of $3.4 \cdot 10^8$ (as defined in *Zhong et al*. [2000]) with temperature scaled such that $d\ln \rho / d\ln VS = 0.2$. This constant scaling is simplified and does not take depth-dependent mineral physics relationships into account [e.g., *Forte*, 2007], nor do we allow for compositional anomalies at deeper levels, such as within the LLSVPs. However, such complications will mainly affect the amplitude but not the geometry of mantle flow [cf. *Gurnis et al*., 2000]. The boundary conditions are shear-stress free at the surface, allowing for dynamically consistent plate motions guided by weak zones prescribed at plate boundaries [*Ricard and Vigny*, 1989; *Zhong et al*., 2000]. To test the role of slab pull, we also consider upper mantle models that either consist of, or have added, slab structure as inferred from Wadati-Benioff zone seismicity, based on the RUM geometry [*Gudmundsson and Sambridge*, 1998; *Ghosh et al*., 2010]. In addition, our models include the effect of the "ridge-push" (i.e., lithospheric thickening) force approximately by accounting for the top 100 km tomography anomalies that contain the half-space oceanic cooling signature of the ocean. A comparison of models with or without that layer (not shown) indicates that this contribution is relatively minor, consistent with results by *Ghosh et al*. [2006] for the India-Asia collision. Driving forces are balanced by the resistance of the lithosphere to viscous deformation, including sliding and bending along plate boundaries, and regionally by the plate's gravitational potential energy (GPE). Incorporating all of these forces in a global circulation model in a consistent way is still a difficult challenge and subject to large uncertainties associated with deformation localization and appropriate choices for rheology [e.g., *Alisic et al*., 2012]. While our models account for viscous dissipation within lithosphere and mantle, the GPE forces related to crustal thickening, which are mainly efficient during the late-stage evolution of an orogen, are not included. Because of the trade-off between GPE and lithosphere deformation, this simplification should not significantly affect our results. The energy dissipation due to viscous bending in subducting slabs is also approximately included for the cases where we include upper mantle slabs and lateral viscosity variations. Moreover, previous tests have shown that this force might not represent a major control on plate motion [*Buffet and Becker*, 2012; *Alisic et al*., 2012; *Di Giuseppe et al*., 2008; *Wu et al*., 2008].

[18] As for the material properties of the lithosphere, plate boundaries, and mantle, we explore a limited parameter space to find the best-fitting lateral viscosity variations within tectonically defined domains (based on 3SMAC) [*Nataf and Ricard*, 1996] that yield a good fit to global plate motions and the geoid, a process akin to "viscous tomography" [cf. *Ghosh et al*., 2010]. For our SMEAN reference model, we find background viscosities for the lithosphere (depth $z \leq 100$ km), upper mantle ($100 < z \leq 660$ km), and lower mantle ($z > 660$ km) viscosities of $1.5 \cdot 10^{23}$, 10^{21}, and $6 \cdot 10^{22}$ Pas, respectively. Within those layers, relative viscosities are 0.01 for weak zones (as defined in *Becker and Faccenna* [2011]), 50 for continental lithosphere ($z \leq 100$ km), 500 for cratonic regions ($z \leq 300$ km), and 0.01 for the suboceanic plate asthenosphere ($100 < z \leq 300$ km). With such plausible lateral viscosity variations, a good fit to plate motions fit can be achieved based on a simple interpretation of tomography.

[19] We could have instead adopted a simpler, only radially varying profile of mantle viscosity [e.g., *Hager*, 1984; *Schubert et al*., 2001], with no attempt to improve the match to the geoid or plate velocities. Sensitivity tests reveal that these simpler viscosity structures modify the details of plate speeds [cf. *Becker and Faccenna*, 2011] and, expectedly, lead to a somewhat poorer match of surface motions. However, these models show the same general relative velocities patterns, and hence lithospheric stresses, as the optimized viscosity models and, importantly, the same general dependency on the density models. This is consistent with findings regarding the presence of a low-viscosity asthenosphere. Such a layer may influence the mutual role between mantle drag and slab pull, but the basic patterns of plate motion are relatively unchanged [*Becker*, 2006; *van Summeren et al*., 2012].

[20] Figure 3 shows results from our reference model with the optimized viscosity structure, which may be compared directly with plate motions (Figure 3d; linear correlation is 0.93) or the geoid (not shown; correlation is 0.78, both computed as in *Ghosh et al*. [2010]). Figure 3d shows that most plate motions are matched fairly well, with the exception of North America and Australia. Importantly, the plate velocity prediction works well for both India-Eurasia and the South America–Nazca convergent margins. Moreover, the general mantle flow patterns described below do not depend strongly on model details, such as the chosen viscosity structure, including additional lateral viscosity variations such as those expected due to temperature-dependent viscosity, which mainly affects the relative velocities of upwellings and downwellings.

[21] Figure 3a shows the mantle flow solution averaged over upper mantle depths. In the southern Atlantic system, flow is rather weak, with an overall eastward motion from Africa, where a remarkable upwelling is focused on Ethiopia-Afar, toward the Cordilleras. At larger depths (1500–2700 km; Figure 3c), flow is reversed with intense flow from the Cordillera to the African low-velocity zone. Hence we may define a large-scale convection cell, running from the Africa low-velocity anomaly to the Cordillera high-velocity feature (Figure 3d), with a N-S trending axis roughly positioned in correspondence to the south Atlantic ridge (Figure 3b; *Husson et al*. [2012]). On the eastern side of Africa, upper mantle flow is trending from the Afar-Carlsberg ridge toward the Tethyan high-velocity anomaly [*Becker and Faccenna*, 2011]. In the upper portion of the lower mantle (Figure 3b), this trend is reversed and gets stronger at larger mantle depth (Figure 3c). Overall, this convection pattern defines a large-scale convection cell with a NW-SE axis running from Arabia to Australia (Figure 3b). While the axis of the Tethyan cell is located in the upper

mantle, the south Atlantic one is deeper and positioned in the midmantle. It is possible that those two cells merge together north of Iceland, enclosing the African LLSVP.

[22] A similar setting may be described for the Pacific superswell. On cross section (Figure 3e), these convection cells form, in conjunction with the other prominent low-velocity zone placed beneath the southwest Pacific, a rather symmetric mantle system dominated by four large convection cells [e.g., *Alvarez*, 1990; *Schubert et al*., 2001; *Romanowicz and Gung*, 2002; *Dziewonski et al*., 2010]. Figure 3d also shows that the SE tip of the Tethyan subduction faces and merges with the Pacific one, at least in the upper middle mantle, forming a broad downwelling zone. Downwellings are characterized by vertical to reclined flow lines in both regions, implying that the trench motion is stationary or advancing. The Andes and the Alpine-Himalayan belt, presently located in correspondence to large-scale, high-velocity features, are indeed positioned on the return limbs of a large-scale convection cell, centered around the African LLSVP. These convection patterns suggest that the plates connected to orogenic buildup are subjected to vigorous mantle tractions (plate suction forces; cf. *Becker and O'Connell* [2001] and *Conrad and Lithgow-Bertelloni* 2002]) that may reach levels of ~6–8 · 10^{12} Nm^{-1} for the case of South America [*Husson et al*., 2012].

3.1. Dependence on Density Models and Style of Mantle Convection

[23] To illustrate the role of the different components of mantle heterogeneity, we vary our density models, leaving all other parameters such as viscosity structures the same. The role of subduction zones and slab pull on plate motions can be tested by assigning density anomalies only to regions where there is Wadati-Benioff zone seismicity (here in the RUM model locations of *Gudmundsson and Sambridge* [1998], as used in *Ghosh et al*. [2010]). The resulting plate motions for flow induced by such slabs alone are shown in Figure 4a. Overall, the direction of motion is matched well [*Becker and O'Connell*, 2001], but the amplitude of the velocity is strongly reduced. The direction of Africa, for example, is correctly reproduced but at reduced speed (~30% of NUVEL-1A). India, conversely, is not matched well and moving slowly eastward, while South America is virtually stationary.

[24] The match between model and plate motions increases when adding lower mantle anomalies from tomography (Figure 4c) and, slightly further, when adding upper mantle "hot" (i.e., seismically slow velocity) anomalies (Figure 4d). Adding density anomalies to upper mantle slabs substantially increases plate velocities and improves the correlations with crustal plate motion. This indicates that overall plate motions are sustained by whole-mantle convection cells driven in part by deep mantle slabs, while the pull of active, upper mantle subduction zones correctly modulates their direction. These examples do not, of course, constitute a comprehensive test (for which we would have had to redo the viscous tomography) and other model assumptions can lead to somewhat different conclusions [*Alisic et al*., 2012]. However, our results substantiate that a correct blend between slab pull and slab suction is able to match plate motions [*Becker and O'Connell*, 2001; *Conrad and Lithgow-Bertelloni*, 2002; *Ghosh et al*., 2010; *Faccenna et al*., 2012; *van Summeren et al*., 2012], and the velocity models are quite robust. For example, correlation with surface motion does not change significantly when temperature-dependent viscosity throughout the mantle, or the top 100 km of tomography are included for density variations in the lithosphere. However, our reference model provides the best fit to the geoid.

4. Evolution of Mantle Flow During Mountain Building

[25] To truly unravel the relationship between the style of convection and mountain building, it is necessary to backtrack mantle flow during orogeny. Reconstructions of convection back in time have been performed for the African superswell [*Conrad and Gurnis*, 2003], for subduction zones using trench motions and tomography [e.g., *Ricard et al*., 1993; *Lithgow-Bertelloni and Richards*, 1998; *Steinberger*, 2000; *Bunge and Grand*, 2000; *Replumaz et al*., 2004; *Hafkenscheid et al*., 2006; *van der Meer et al*., 2010], and in regional settings using geological fingerprints [e.g., *Gurnis*, 1993; *Pysklywec and Ishii*, 2005; *Liu et al*., 2008]. However, properly incorporating the interactions of descending slabs with the phase transitions around the 660 km discontinuity in global models remains a challenge, and existing convective forward models of the global subduction system match seismic tomography only at the longest wavelengths [*Becker and Boschi*, 2002].

4.1. Trench Motion and Slab Penetration Into Lower Mantle

[26] Here we reconstruct positions of the Nazca-Farallon-South America and Eurasia-Tethyan plate boundaries over the last 90 Myr and compare them with high-velocity anomalies in the mantle to constrain the timing and position for the accumulation of subducted material in the upper/lower mantle transition at 660 km. Plate reconstructions are performed using the GPlates software adopting the *Müller et al*. [2008] kinematic model [see also *Sdrolias and Müller*, 2006], assuming that slab anomalies sink vertically in the lower mantle [*Ricard et al*., 1993; *van der Meer et al*.,

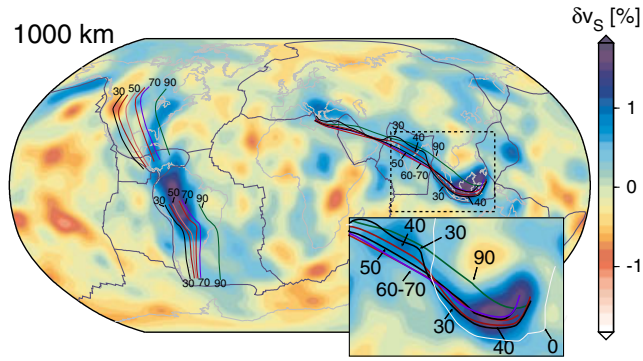

Figure 5. Location of trench over time plotted on top of SMEAN composite tomography at 1000 km depth. The position of trench is calculated using the *Müller et al*. [2008] absolute reference frame. Note that trenches line up with deep mantle anomalies at ~50–60 Ma both for the Cordillera and the Indonesia-Indian slab.

2010]. For the durations we consider, a few tens of million years, this approximation should hold, to first order.

[27] High-velocity anomalies beneath the Tethyan belt extend from Indonesia to the Aegean, penetrating into the lower mantle down to a depth of 1500–1600 km [*van der Voo et al*., 1999; *Kárason and van der Hilst*, 2000; *Replumaz et al*., 2004; *Hafkenscheid et al*., 2006; *Li et al*., 2008]. Previous estimates of the age of penetration of the slab beneath Java based on tectonic reconstruction gives ~50 Ma [*Replumaz et al*., 2004], or ~40 Ma based on subduction modeling [*Kárason and van der Hilst*, 2000]. *Goes et al*. [2008] correlate the Australian plate acceleration between 60 and 50 Ma with lower mantle subduction. Inspection of Figure 5 reveals that beneath Java the high-velocity body at ~1000–1300 km is positioned ~10° north of the present trench, beneath the back-arc region. As the trench migrated southward through time, its past location may give an indication of the maximum age of penetration. Figure 5 shows that the trench is positioned north of the deep anomaly from 90 to 70 Ma, just on top of the anomaly from 70 to 60 Ma, and it lines up with it from ~40 Ma. This test supports previous estimates, suggesting that slab penetration in the lower mantle could not be older than ~50 Ma. The deep Indonesia anomaly lines up with the Indian one, commonly attributed to Neo-Tethys lithosphere [*van der Voo et al*., 1999] or Spongtang back-arc lithosphere [*Hafkenscheid et al*., 2006]. On the basis of the reconstructed lower mantle subduction velocity, *Replumaz et al*. [2004] established that initial penetration into the lower mantle probably initiated at ~65 Ma. Our results in Figure 5 are not inconsistent with this interpretation, as the position of the northern Indian margin lines up with the deep lower mantle anomaly at a depth of 1000 km at ~50–60 Ma. *van Hinsbergen et al*. [2011b] and *Cande and Stegman* [2011] discuss the acceleration of the Indian in the context of a mantle upwelling, as attested by the Deccan LIP emplacement, presumably related to the Réunion hot spot. On the basis of previous reconstructions, we additionally suggest that the upwelling at that time was contemporaneous with large-scale downwellings due to slab descent into the lower mantle between ~65 and 55 Ma, introducing punctuated mantle flow and plate motion speed-up after a period of relative deep mantle stagnation and slab ponding at 660 km. Subduction at that time will be associated with contemporaneous return flow upwellings, and perhaps localized plume activity as attested by the emplacement of the Deccan LIP [*van Hinsbergen et al*., 2011b].

[28] The westernmost tip of the Tethyan fast velocity anomaly lies beneath the currently active Hellenic subduction. *Faccenna et al*. [2003] backtracked the position of the Aegean trench with respect to the deep anomaly and concluded that the entrance of the slab into the lower mantle occurred in the early Tertiary, after stagnation of subducted material on the 660 km discontinuity for ~20 Myr. *van Hinsbergen et al*. [2005] confirmed this prediction, and *Capitanio et al*. [2009] use the stretching event recorded in the Sirte Gulf to bracket an avalanching episode at ~70 Ma, peaking at ~50 Ma, and then rapidly fading.

[29] In agreement with previous reconstructions, the fit between trench position and mantle velocity anomaly shows that the Tethyan high-velocity anomaly, extending from the central Mediterranean to Indonesia at a depth between ~1000 and 1500 km, started to penetrate the lower mantle from ~65–60 Ma to at least ~45 Ma. Considering the inherent errors in such reconstructions, it is difficult to establish if there is a diachronous evolution and if penetration occurred gradually or by a more punctuated avalanching. Penetration of the slab into the lower mantle does appear to correspond to the outpouring of the Deccan LIP and to the speed-up of the Indian plate along with the spreading rate increase of the Indian Ocean [*Conrad and Lithgow-Bertelloni*, 2007]. Our reconstruction is unable to predict if new material is presently penetrating the 660 km discontinuity.

[30] The Cordillera high-velocity zone represents the other prominent feature extending from Canada to South America, vanishing south of Bolivia. In the northern Cordillera, the reconstruction is complicated by the Laramide flat slab episode. The high-velocity structure extends over the Great Lakes region, sharply bending, probably as a result of the Kula-Farallon plate boundary [*Bunge and Grand*, 2000]. From subsidence analysis, the descent of the flat slab started at ~70 Ma, slowly penetrating in the lower mantle after 60 Ma [*Liu et al*., 2008, 2010]. Beneath central-northern South America, the fast seismic feature is more prominent, showing an apparent continuous slab from the upper to the lower mantle [*van der Hilst et al*., 1997; *Bijwaard et al*., 1998; *Ren et al*., 2007]. On the basis of kinematic arguments, *Goes et al*. [2008] propose that deep penetration beneath central America occurred at ~55–45 Ma. Over south-central America, the trench retreated westward during the opening of the Atlantic. Figure 5 shows that the trench lines up with the high-velocity anomaly at ~50–40 Ma. Summing up, it is most probable that the slab entered the lower mantle not before ~50–40 Ma underneath the Cordilleras.

[31] From the overall reconstruction we may interpret these regional slab penetration events to be of smaller scale than the near-global avalanching events seen in earlier, strongly negative 660 km Clapeyron-slope geodynamic models [e.g., *Machetel and Weber*, 1991; *Tackley et al*., 1993; *Solheim and Peltier*, 1994; *Pysklywec and Mitrovica*, 1997; *Brunei and Machetel*, 1997]. Regional penetration events have been proposed along the western and eastern Pacific, for example, for Tonga and the Marianas [*van der Hilst and Seno*, 1993; *Pysklywec et al*., 2003] and Central America [*Goes et al*., 2008; *van der Hilst et al*., 1997], to reconcile plate tectonic with mantle tomography. Regional analogue and numerical modeling supports the possibility of slab penetration, after slab stagnation on the 660 km discontinuity for some millions of years [e.g., *Kincaid and Olson*, 1987; *Zhong and Gurnis*, 1995; *Griffiths et al*., 1995; *Gouillou-Frottier et al*., 1995; *Christensen*, 1996; *Ita and King*, 1998; *Pysklywec and Ishii*, 2005], with accompanying excitation of surface plate motions and mantle convection.

4.2. African Upwelling

[32] We infer that those deep subduction episodes on the outer sides of the convective cells are likely correlated with major upwelling episodes in the center, which is beneath the Indo-African plate. The African and Indian plates indeed show widespread evidence of uplift and intraplate volcanism [*Cox*, 1989; *Burke*, 1996]. During the Tertiary, the main upwelling episode may be associated with the outpouring of the Deccan trap at ~65.5 Ma [e.g., *Allegre et al*., 1999], perhaps related to the Réunion plume [*Cande and Stegman*, 2011; *van Hinsbergen et al*., 2011b], and by the Ethiopian trap from

~45 Ma onward [*Ebinger et al*., 1993; *Hoffman et al*., 2000]. The outpouring of the Ethiopian basalts started in the south at ~45–40 Ma [*Ebinger et al*., 1993] while the main eruptive phase is at ~30 Ma [*Hoffman et al*., 2000]. *Burke* [1996] suggested that it was the relatively slow motion of the African plate from ~35 Ma onward during this younger eruptive phase that allowed for the mantle upwelling to be expressed as anomalous elevation and volcanism. This includes the emplacement of a dozen hot spots, like Tibesti, Darfur, Hoggar, Adamawa, and all the other eruptive centers scattered near the East African rift zone. *Ebinger and Sleep* [1998] show that a large, single plume impinging at ~45 Ma beneath the Ethiopian plateau is able to match the distribution of volcanism over most of those sites.

[33] The other evidence for a mantle upwelling is the potentially dynamically supported topography of South Africa [*Lithgow-Bertelloni and Silver*, 1998; *Gurnis et al*., 2000] that may have also caused the formation of the plateau, which stands at an elevation of ~1 km. Part of this uplift should have been generated in the last 30–20 Myr [*Partridge and Maud*, 1987; *Partridge*, 1997], as also documented by an Oligocene unconformity along the South African Escarpment [*Burke*, 1996]. Inverted river profiles from a series of African topographic swells—e.g., South African, Namibian, Hoggar, and Tibesti domes—suggest that these domes grew rapidly during the last 30–40 Myr [*Roberts and White*, 2010]. However, geological constraints on both age and rate of uplift are still uncertain, and the present-day river patterns and divide distributions contrast with a "domal shape" uplift expected from mantle upwellings [*Moore et al*., 2009]. In addition, recent dynamic topography models show that expected uplift of southern Africa might be reduced in the presence of ubiquitous chemical mantle heterogeneities [*Moucha and Forte*, 2011]. Hence evidence of a mantle upwelling in Africa-India is mainly related to the extensive volcanism and domal uplift showing two main pulses. The first appeared over the Réunion plume, producing the Deccan LIP at ~63 Ma and then moved over central Africa, centered in Ethiopia. Here magmatism started probably at ~45 Ma, peaking around ~30 Ma, and lasting up to the present [*Burke*, 1996].

5. Discussion: Role of Mantle Convection on Mountain Building

[34] Mountain belts are intimately related to mantle convection [*Collins*, 2003]. Models of the present-day pattern of mantle convection indicate that the basal mantle drag exerted by whole-mantle convection cells produces the necessary propulsion to explain plate motions and to produce the stresses at plate boundaries necessary to build up mountains. Such convective "conveyor belts" [*Becker and Faccenna*, 2011] appear a necessary condition for India to keep advancing toward Eurasia, for example. Underneath the Andes, flow lines are near vertical in the subduction zone, indicating that the overall suction due to a large-scale downwelling anchors the trench while pulling the Americas westward (Figure 6a).

[35] Geological data and plate reconstructions are consistent with our suggestion that mountain building and crustal thickening occurred once slabs penetrated into the lower mantle after phases of stagnation at 660 km. Penetration appears to have initiated in two pulses, possibly at ~65–55 Ma in the Tethyan and later at ~50–40 Ma in the Cordillera. These subduction episodes generated the fast-velocity anomalies that are presently found beneath the Cordilleras and the Himalayas at midmantle depths of ~1000–1400 km, presumably still sinking, with an average speed of ~1–1.5 cm/yr [*van der Meer et al*., 2010].

[36] The onset of crustal thickening and uplift of these orogenic belts corresponds to, or slightly postdates, these episodes of slab penetration, and the establishment of the present-day, whole-mantle convection cell structure. In the Andes the onset of slab penetration into the lower mantle likely occurred at ~50 Ma. Slab penetration into the higher-viscosity lower mantle should be an efficient mechanism to anchor the slab and to impede its lateral migration and trench motions (Figure 6b). This would result in the growth of compressional stresses between the advancing South America plate and the stationary Nazca trench [*Husson et al*., 2012]. For the case of Himalaya-Tibet, most models propose that the onset of collision started at ~55–50 Ma because of the arrival of the Indian continent on the subduction zone. If our model is correct, we could have mountain building even without having a continent-continent collision, just because deep lower mantle subduction anchors slab and opposes trench rollback. Indeed, more recent models for Tibet propose a two-stage collisional process [*van Hinsbergen et al*., 2012] with the more intense collisional phase at ~25–20 Ma [*Aitchison et al*., 2007].

[37] The two episodes of slab penetration for Tibet and the Andes also correlate fairly well with the signatures of mantle upwellings. For the Indian-Himalaya system, the bottom-up connections appear fairly clear: our reconstructions indicate that the Tethyan slab initiated its journey into the lower mantle at the time the Deccan trap was emplaced. For the South Atlantic system, the correlation is more ambiguous. As indicated by the present-day patterns, the return flow from the Nazca slab is beneath Africa (Figure 2c). The Ethiopian traps initiated at ~45 Ma, contemporaneous with, or soon after, the penetration of the Nazca slab in the lower mantle. The establishment of a vigorous convection cell on both sides of the superswell is, however, strongly suggested by the acceleration of the associated midoceanic spreading rates. The timing of the inferred upwelling and downwelling support the idea that the present-day cell activated in the early Tertiary, probably after a critical mass of slab material accumulated on the 660 km discontinuity. From the reconstructions, it is not possible to determine if active upwellings drive downwellings or vice versa, and the two are clearly just two aspects of the same convective system. We are left to speculate that if upwellings were driving downwellings, we would expect a contemporaneous acceleration of the two convection cells. Instead they are separated by ~15 Ma, implying that the role of deep slab dynamics is more important in establishing the convective cells.

[38] The anticorrelation between spreading rates in the Indian and South Atlantic oceans also suggests a linkage between the motion of India, Africa, and South America within an Indo-Atlantic cell [*Davaille et al*., 2005]. Based on seafloor reconstructions, *Cande and Stegman* [2011] proposed that the upwelling of the Réunion plume at ~65 Ma propelled India at high speeds against Eurasia [*Gurnis and Torsvik*, 1994] and produced slow motion of Africa toward the W/NW, causing a slowdown of the Atlantic

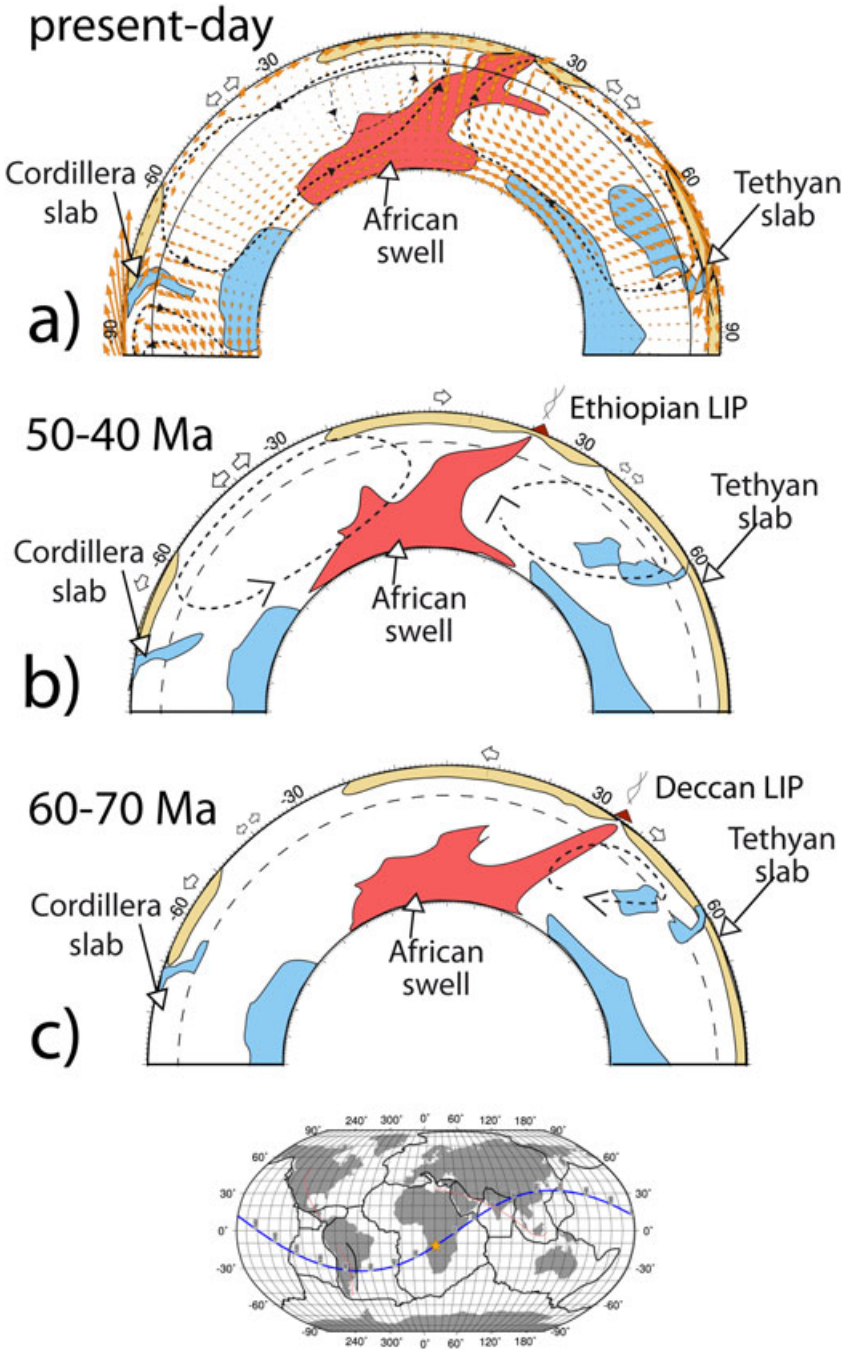

Figure 6. Three-stage model for the convection scenario occurring at present day (deduced from Figure 2d) and at 60 Ma. The evolution of the low-velocity zone is inferred from *Conrad and Gurnis* [2003].

spreading rate. However, the effect of a plume may not be sufficient to explain sustained plate speed-up [*van Hinsbergen et al.*, 2011b]. Alternatively, it could be that the collisional slow down of India at ~50 Ma blocked the expansion of the system on the eastern side of the African superswell. Instead the surface expression of the accelerated African upwelling transferred to the opposite western side, re-establishing of the South Atlantic spreading rate.

[39] The sequence of processes illustrated here suggests to us that the regional amplification of the effects of whole-mantle flow is necessary to create significant mountains and to sustain the required compressive forces in the lithosphere. The impact of slab avalanching in triggering a conveyor belt that rams plates against each other is in principle measurable by comparing the model flow induced by downwellings only, in the upper mantle, to that induced by downwellings only, in the entire mantle. Indeed, a variety of models confirm this view [e.g., *Pysklywec and Mitrovica*, 1997; *Pysklywec et al.*, 2003; *Zhong and Gurnis*, 1995; *Machetel and Weber*, 1991]. We deduce that mantle tractions are necessary to efficiently drag plates against each other, overcoming the resisting forces such as the increase of

potential energy of the rising mountain belt. If our model holds, it should then possible to use global-scale orogenic processes, such as those occurring during supercontinental assembly, as diagnostic of pulses of whole-mantle convection. *Cawood and Buchan* [2007] distinguished accretionary from collisional orogens that formed during the final assembly of Gondwanaland (between ~570 and ~520 Ma, including the east African orogen and Mozambique belt and the Kuunga, Pinjarra, and Brasiliano orogens) and Pangea supercontinent between ~320 and ~250 Ma, generating the Appalachian, Variscan, and Urals orogens [*Stampfli and Borel*, 2002]. *Cawood and Buchan* [2007] proposed that accretionary orogens formed at the periphery of supercontinents while collisional orogens form in the interior, possibly along existing suture zones. In agreement with this view we suggest that the supercontinental cycle may reflect periods of intense plate convergence driven by episodes of slab avalanching, perhaps in relation to the convective settings induced by the time-variable continental cover.

[40] Previous studies also proposed that the mid-Cretaceous breakup of Gondwana and the formation of oceanic plateaus in the central Pacific and Indian Ocean basins may have been triggered by large-scale avalanching of slab material into the lower mantle [*Larson and Kincaid*, 1996]. Here we provide a detailed convection history related to smaller-scale episodes of regional miniavalanches that can be associated with a small number of individual plumes [*Condie*, 1998] connected to the large-scale superswell structure [*Davaille et al*., 2005]. If this model is correct, it would be possible to interpret the Wilson cycle in the light of slab penetration, relating cycles of continental assembly with episodes of slab avalanching. For example, the present-day setting of the southern Atlantic, where large-scale convection is producing overall in-plane compression, could eventually lead to passive margin inversion, i.e., subduction initiation. We would then expect the slab-pull type orogeny to form at first, eventually evolving into the slab-suction, collisional type of orogeny.

[41] This "bottom up" tectonic model proposed here sheds new light on the style of back-arc deformation and mountain building. This can be illustrated by the Pacific dichotomy: in the western margins, slabs are mainly restricted to the upper mantle, which leads mainly to back-arc extension due to slab-pull-induced trench retreat. In the eastern Pacific Bolivian orocline or the Tethyan slab, deep slab anchoring is producing thick crustal piles and orogeny. The transition between those cases would be represented by "slab pull" orogeny. Such slab pull orogenic belts are characterized by an asymmetric wedge, with a low, tapered prowedge such that crustal thickening does not exceed a certain value (~40 km), as it is being continuously reduced by low-angle, extensional detachments producing exhumation of deep units.

[42] Slab pull types of mountains are generally occurring over areas where slabs are transiently ponding on 660 km, and convection is temporarily confined to the upper mantle. This could apply to the Mediterranean style mountain belts, from the Betics to the Apennines and Hellenides or the Carpathians [*Royden*, 1993a]. We may include in this class also the southern Andean belt of Patagonia and the Zagros. This class of orogen may evolve into the "slab suction" orogeny if deep convection is modified by slab penetration into the lower mantle. In this case, slab suction and upwellings due to a whole-mantle convection cell are dragging plates against each other toward the zone of deep mantle downwellings, and ensuring prolonged convergence independently on the nature of the subducting material [*Alvarez*, 2010]. This second type of orogen, exemplified by the Tibet-Himalayan orogen and the Puna-Altiplano, is doubly vergent, and characterized by large crustal thickening with the volcanic arc centered within the orogen. Over these belts, exhumation of deep high-pressure units is often very reduced, if found at all, or most of the process is dominated by high Moho temperatures. If this model is correct, crustal thickening may be a direct function of the depth and vigor of mantle convection (Figure 7).

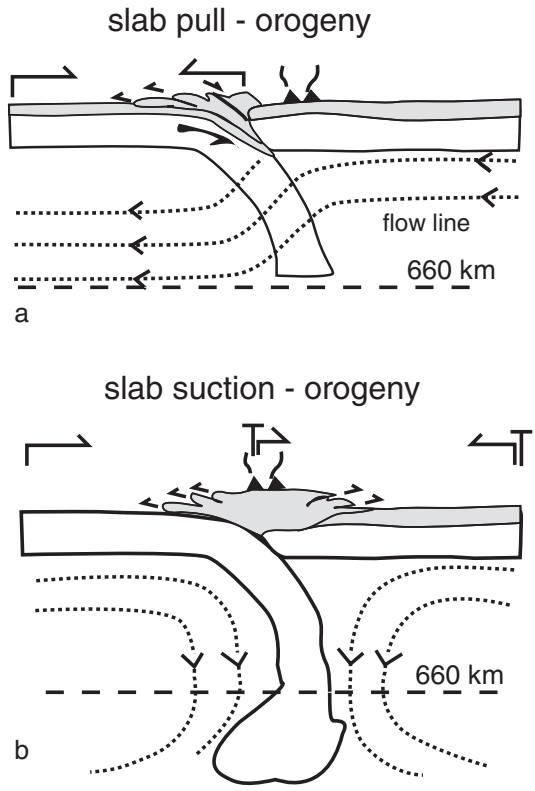

Figure 7. Model of orogenic buildup (modified from and inspired by *Conrad and Lithgow-Bertelloni* [2002]). Mode (a) orogenic wedge may grow asymmetrically due to the accretion of crustal slices. In the inner portion of the wedge, extensional detachment may produce exhumation of high-pressure units on the surface. This type of orogen may form during trench rollback, symptomatic of efficient, one-sided slab pull, preventing crustal thickening. Flow lines inferred from *Funiciello et al*. [2006] and *Becker and Faccenna* [2011]. Mode (b) orogenic growth with strong crustal thickening formed by advancing (Asia/Himalaya case) or stationary (South America/Andes case) trench against a stationary (Asia) or advancing upper plate (South America). In these regions, downwelling can be traced down into the lower mantle, generating a suction force that drag plates in collision.

6. Conclusion

[43] Orogeny is inferred to fall into two end-members, the slab pull and slab suction cases. The former appears associated

with transiently ponding slabs whose upper mantle convective style is associated with trench rollback and the formation of mountains with moderate crustal thickness such as in the Mediterranean. The latter case is associated with slabs penetrating through the phase transitions around 660 km, leading to symmetric convergence, and the formation of mountains with thick (>50 km) crustal columns. For the slab suction type of orogeny, the resulting whole-mantle convection cells not only establish conveyor belts for the intense compressive forces needed for continental collisions, but also lead to associated upwellings, and we trace the geological evidence for this downwelling-upwelling link for the cases of the Andes and the Himalayas. A variety of transitional forms of orogens will exist between those two end-members such as the Zagros or the Alps along the Tethys or the Sevier-Laramides along the Cordillera. If our model is correct, we can use the geological evolution of orogenic belts to decipher the scale and the evolving style of mantle convection.

[44] **Acknowledgments.** This manuscript benefited from the comments of Chris Beaumont and an anonymous reviewer as well as from suggestions by Editor Onno Oncken. Discussions Jean Pierre Brun contributed clarified some of the concepts expressed here, and we thank A. Ghosh for earlier help with input model construction. We thank CitcomS authors, including S. Zhong, E. Tan, A. McNamara, and L. Moresi for their contributions, CIG (geodynamics.org), and seismologists who share their models in electronic form. Computations were performed on USC's High Performance Computing Center, and research was supported by NSF grants EAR-0855546 (C.P.C.), EAR 0930046, and 0643365 (T.W.B.).

References

Aitchison, J. C., J. R. Ali, and A. M. Davis (2007), When and where did India and Asia collide?, *J. Geophys. Res.*,*112*, B05423, doi:10.1029/2006JB004706.

Alisic, L., M. Gurnis, G. Stadler, C. Burstedde, and O. Ghattas (2012), Multiscale dynamics and rheology of mantle flow with plates, *J. Geophys. Res.*, *117*, B10402, doi:10.1029/2012JB009234.

Allegre, C. J., J. L. Birck, F. Capmas, and V. Courtillot (1999), Age of the Deccan traps using ^{187}Re–^{187}Os systematics, *Earth Planet. Sci. Lett.*, *170*, 197–204.

Alvarez, W. (1990), Geologic evidence for the plate-driving mechanism: The continental undertow hypothesis and the Australian-Antarctic Discordance, *Tectonics*, *9*, 1213–1220.

Alvarez, W. (2010), Protracted continental collisions argue for continental plates driven by basal traction, *Earth Planet. Sci. Lett.*, *296*, 434–442.

Bardintzeff, J.-M., J.-P. Liégois, B. Bonin, H. Bellon, and G. Rasamimanana (2010), Madagascar volcanic provinces linked to the Gondwana break-up: Geochemical and isotopic evidences for contrasting mantle sources, *Gondwana Res.*, *18*, 295–314.

Becker, T. W. (2006), On the effect of temperature and strain-rate dependent viscosity on global mantle flow, net rotation, and driving forces, *Geophys. J. Int.*, *167*, 943–957.

Becker, T. W., and C. Faccenna, (2011), Mantle conveyor beneath the Tethyan collisional belt, *Earth Planet. Sci. Lett.*, *310*, 453–461.

Becker, T. W., and R. J. O'Connell (2001), Predicting plate velocities with mantle circulation models, *Geochem. Geophys. Geosyst.*, *2*(12), 1060, doi:10.1029/2001GC000171.

Becker, T., and L. Boschi (2002), A comparison of tomographic and geodynamic mantle models, *Geochem. Geophys. Geosyst.*, *3*, 1003, doi:10.1029/2001GC000168.

Bijwaard, H., W. Spakman, and E. Engdahl (1998), Closing the gap between regional and global travel time tomography, *J. Geophys. Res.*, *103*, 30,055–30,078.

Brun, J.-P., and C. Faccenna (2008), Exhumation of high-pressure rocks driven by slab rollback, *Earth Planet. Sci. Lett.*, *272*, 1–7, doi:10.1016/j.epsl.2008.02.038.

Brunei, D., and P. Machetel (1997), Large-scale tectonic features induced by mantle avalanches with phase, temperature, and pressure lateral variations of viscosity, *J. Geophys. Res.*, *103*, 4929–4945.

Buffett, B. A., and T. W. Becker (2012), Bending stress and dissipation in subducted lithosphere, *J. Geophys. Res.*, *117*, B05413, doi:10.1029/2012JB009205.

Bunge, H.-P., and S. P. Grand (2000), Mesozoic plate-motion history below the northeast Pacific Ocean from seismic images of the subducted Farallon slab, *Nature*, *405*, 337–340.

Bunge, H.-P., M. A. Richards, C. Lithgow-Bertelloni, J. R. Baumgardner, S. P. Grand, and B. A. Romanowicz (1998), Time scales and heterogeneous structure in geodynamic Earth models, *Science*, *280*, 91–95.

Burke, K. (1996), The African plate, *S. Afr. J. Geol.*, *99*, 341–409.

Burke, K., and T. H. Torsvik (2004), Derivation of large igneous provinces of the past 200 million years from long-term heterogeneities in the deep mantle, *Earth Planet. Sci. Lett.*, *227*, 531–538.

Cande, S. C., and D. R. Stegman (2011), Indian and African plate motions driven by the push force of the Reunion plume head, *Nature*, *475*, 47–52.

Capitanio, F. A., C. Faccenna, and R. Funiciello (2009), The opening of Sirte basin: Result of slab avalanching?, *Earth Planet. Sci. Lett.*, *285*, 210–216, doi:10.1016/j.epsl.2009.06.017.

Capitanio, F. A., G. Morra, S. Goes, R. F. Weinberg, and L. Moresi (2010), India-Asia convergence driven by the subduction of the Greater Indian continent, *Nat. Geosci.*, *3*, 136–139.

Cawood, P. A., and C. Buchan (2007), Linking accretionary orogenesis with supercontinent assembly, *Earth Sci. Rev.*, *82*, 217–256.

Chemenda, A. I., J. P. Burg, and M. Mattauer (2000), Evolutionary model of the Himalaya-Tibet system: Geopoem based on new modelling, geological and geophysical data, *Earth Planet. Sci. Lett.*, *174*, 397–409.

Christensen, U. R. (1996), The influence of trench migration on slab penetration into the lower mantle, *Earth Planet. Sci. Lett.*, *140*, 27–39.

Collier, J. S., V. Sansom, O. Ishikuza, R. N. Taylor, T. A. Minshull, and R. B. Whitmarsh (2008), Age of Seychelles–India break-up, *Earth Planet. Sci. Lett.*, *272*, 264–277.

Collins, W. J. (2003), Slab pull, mantle convection, and Pangean assembly and dispersal, *Earth Planet. Sci. Lett.*, *205*, 225–237.

Condie, K. C. (1998), Episodic continental growth and supercontinents: A mantle avalanche connection?, *Earth Planet. Sci. Lett.*, *163*, 97–108.

Conrad, C. P., and M. Gurnis (2003), Seismic tomography, surface uplift, and the breakup of Gondwanaland: Integrating mantle convection backwards in time, *Geochem. Geophys. Geosyst.*, *4*, 1031, doi:10.1029/2001GC000299.

Conrad, C. P., and C. Lithgow-Bertelloni (2002), How mantle slabs drive plate tectonics, *Science*, *298*, 207–209.

Conrad, C. P., and C. Lithgow-Bertelloni (2007), Faster seafloor spreading and lithosphere production during the mid-Cenozoic, *Geology*, *35*, 29–32.

Copley, A., J.-P. Avouac, and J.-Y. Royer (2010), India-Asia collision and the Cenozoic slowdown of the Indian plate: Implications for the forces driving plate motions, *J. Geophys. Res.*, *115*, B03410, doi:10.1029/2009JB006634.

Cox, K. G. (1989), The role of mantle plume in the development of continental drainage pattern, *Nature*, *342*(21/28), 873–876.

Davaille, A., E. Stutzmann, G. Silveira, J. Besse, and V. Courtillot (2005), Convective patterns under the Indo-Atlantic, *Earth Planet. Sci. Lett.*, *239*, 233–252.

DeMets, C., R. G. Gordon, D. F. Argus, and S. Stein (1994), Effect of recent revisions to the geomagnetic reversal time scale on estimates of current plate motions, *Geophys. Res. Lett.*, *21*, 2191–2194.

Dercourt, J., et al. (1986), Geological evolution of the Tethys belt from the Atlantic to the Pamirs since the Lias, *Tectonophysics*, *123*, 241–315.

Dewey, J. F., and J.M. Bird (1970), Mountain belts and the new global tectonics, *J. Geophys. Res.*, *75*, 2625–2647.

Dewey, J. F., M. L. Helman, E. Torco, D. H. W. Hutton, and S. Knott (1989), Kinematics of the western Mediterranean, *Geol. Soc. Spec. Publ.*, *45*, 265–283.

Di Giuseppe, E., J. van Hunen, F. Funiciello, C. Faccenna, and D. Giardini (2008), Slab stiffness control of trench motion: Insights from numerical models, *Geochem. Geophys. Geosyst.*, *9*, Q02014, doi:10.1029/2007GC001776.

Doglioni, C., P. Harabaglia, S. Merlini, F. Mongelli, A. Peccerillo, and C. Piromallo (1999), Orogens and slabs vs their direct of subduction, *Earth Sci. Revs.*, *45*, 167–208.

Dziewonski, A. M, V. Lekic, and B. A. Romanowicz (2010), Mantle anchor structure: An argument for bottom up tectonics, *Earth Planet Sci. Lett.*, *299*, 69–79.

Eagles, G., and M. König (2008), A model of plate kinematics in Gondwana breakup, *Geophys. J. Int.*, *173*, 703–717.

Ebinger, C., and N. Sleep (1998), Cenozoic magmatism throughout East Africa resulting from impact of a single plume, *Nature*, *395*, 788–791.

Ebinger, C., T. Yemane, G. Wolde Gabriel, and J. Aronson (1993), Late Eocene-recent volcanism and faulting in the southern Main Ethiopian rift system, *J. Geol. Soc. London*, *150*, 99–108.

Faccenna, C., L. Jolivet, C. Piromallo, and A. Morelli (2003), Subduction and the depth of convection in the Mediterranean mantle, *J. Geophys. Res.*, *108*(B2), 2099, doi:10.1029/2001JB001690.

Faccenna, C., O. Bellier, J. Martinod, C. Piromallo, and V. Regard (2006), Slab detachment beneath eastern Anatolia: A possible cause for the formation of the North Anatolian fault, *Earth Planet. Sci. Lett.*, *242*, 85–97.

Faccenna, C., T. W. Becker, S. Lallemand, and B. Steinberger (2012), On the role of slab pull in the Cenozoic motion of the Pacific plate, *Geophys. Res. Lett.*, *39*, L03305, doi:10.1029/2011GL050155.

Forte, A.M. (2007), Constraints on seismic models from other disciplines—Implications for mantle dynamics and composition, in *Treatise on Geophysics*, edited by G. Schubert and D. Bercovici, pp. 805–858, Elsevier, Amsterdam, Netherlands.

Funiciello, F., M. Moroni, C. Piromallo, C. Faccenna, A. Cenedese, and H. A. Bui (2006), Mapping mantle flow during retreating subduction: Laboratory models analyzed by feature tracking, *J. Geophys. Res.*, *111*, B03402, doi:10.1029/2005JB003792.

Gaina, C., D. Muller, B. Brown, T. Ishihara, and S. Ivanov (2007), Breakup and early seafloor spreading between India and Antarctica, *Geophys. J. Int.*, *170*, 151–170.

Garfunkel, Z., C. A. Anderson, and G. Schubert (1986), Mantle circulation and the lateral migration of subducted slabs, *J. Geophys. Res.*, *91*, 7205–7223.

Garnero, E. J., and A. K. McNamara (2008), Structure and dynamics of the Earth's lower mantle, *Science*, *320*, 626–628.

Ghosh, A., W. E. Holt, L. M. Flesch, and A. J. Haines (2006), Gravitational potential energy of the Tibetan Plateau and the forces driving the Indian plate, *Geology*, *34*, 321–324.

Ghosh, A., T. W. Becker, and S. Zhong (2010), Effects of lateral viscosity variations on the geoid, *Geophys. Res. Lett.*, *37*, L01301, doi:10.1029/2009GL040426.

Gnos, E., A. Immanhauser, and T. Peters (1997), Late Cretaceous/early Tertiary convergence between the Indian and Arabian plates recorded in ophiolites and related sediments, *Tectonophysics*, *271*, 1–19.

Goes, S., F. A. Capitanio, and G. Morra, (2008), Evidence of lower mantle slab penetration phases in plate motions, *Nature*, *451*, 981–984.

Gouillou-Frottier, L, J. Buttles, and P. Olson (1995), Laboratory experiments on the structure of subducted lithosphere, *Earth Planet. Sci. Lett.*, *133*, 19–34.

Grand, S. P., R. D. van der Hilst, and S. Widiyantoro (1997), High resolution global tomography a snapshot of convection in the Earth, *Geol. Soc. Am. Today*, *7*, 1–7.

Griffiths, R. W., R. I. Hackney, and R. D. van der Hilst (1995), A laboratory investigation of effects of trench migration on the descent of subducted slabs, *Earth Planet. Sci. Lett.*, *133*, 1–17.

Gudmundsson, O., and M. Sambridge, (1998), A regionalized upper mantle (RUM) seismic model, *J. Geophys. Res.*, *103*, 7121–7136.

Guillot, S., E. Garzanti, D. Baratoux, D. Marquer, G. Mahéo, and J. de Sigoyer (2003), Reconstructing the total shortening history of the NW Himalaya, *Geochem. Geophys. Geosyst.*, *4*, 1064, doi:10.1029/2002GC000484.

Gurnis, M. (1993), Phanerozoic marine inundation of continents driven by dynamic topography above subducting slabs, *Nature*, *364*, 589–593.

Gurnis, M., and T. Torsvik, (1994), Rapid drift of large continents during the Late Precambrian and Paleozoic: Paleomagnetic constraints and dynamics models, *Geology*, *22*, 1023–1026.

Gurnis, M., J. X. Mitrovica, J. Ritsema, and H.-J. van Heijst (2000), Constraining mantle density structure using geological evidence of surface uplift rates: The case of the African superplume, *Geochem. Geophys. Geosyst.*, *1*(7), 1020, doi:10.1029/1999GC000035.

Hafkenscheid, E., M. J. R. Wortel, and W. Spakman (2006), Subduction history of Tethyan region derived from seismic tomography and tectonic reconstructions, *J. Geophys. Res.*, *111*, B08401, doi:10.1029/2005JB003791.

Hager, B. H. (1984), Subducted slabs and the geoid: Constraints on mantle rheology and flow, *J. Geophys. Res.*, *89*(B7), 6003–6015, doi:10.1029/JB089iB07p06003.

Hager, B. H., and R. W. Clayton (1989), Constraints on the structure of mantle convection using seismic observations, flow models, and the geoid, in *Mantle Convection*: *Plate Tectonics and Global Dynamics*, *The Fluid Mechanics of Astrophysics and Geophysics*, edited by W. R. Peltier, *4*, pp. 657–763, Gordon and Breach, New York.

Hatzfeld, D., and P. Molnar, (2010), Comparisons of the kinematics and deep structures of the Zagros and Himalaya and of the Iranian and Tibetan plateaus and geodynamic implications, *Rev. Geophys.*, *48*, RG2005, doi:10.1029/2009RG000304.

Hofmann, C., G. Feraud, and V. Courtillot (2000), 40Ar/39Ar dating of mineral separates and whole rocks from the Western Ghats lava pile: Further constraints on duration and age of the Deccan traps, *Earth Planet. Sci. Lett.*, *180*, 13–27.

Husson, L., and Y. Ricard (2004), Stress balance above subduction zones—Application to the Andes, *Earth Planet. Sci. Lett.*, *222*, 1037–1050.

Husson, L., P. C. Conrad, and C. Faccenna, (2012), Plate motions, Andean orogeny, and volcanism above the South Atlantic convection cell, *Earth Planet. Sci. Lett.*, *317–318*, 126–135.

Ita, J., and S. D. King (1998), The influence of thermodynamic formulation on simulations of subduction zone geometry and history, *Geophys. Res. Lett.*, *25*, 1463–1466.

Jolivet, L., C. Faccenna, B. Goffé, E. Burov, and P. Agard (2003), Subduction tectonics and exhumation of high-pressure metamorphic rocks in the Mediterranean orogens, *Am. J. Sci.*, *303*, 353–409, doi:10.2475/ajs.303.5.353.

Jourdan, F., G. Feraud, H. Bertrand, and M. K. Watkeys (2007), From flood basalts to the inception of oceanization: Example from the 40Ar/39Ar high-resolution picture of the Karoo large igneous province. *Geochem. Geophys. Geosyst.*, *8*, Q02002, doi:10.1029/2006GC001392.

Kárason, H., and R. D. van der Hilst, (2000), *Constraints on Mantle Convection From Seismic Tomography, Geophys. Monogr. Ser.*, edited by M. A. Richards, R. G. Gordon, and R. D. van der Hilst, vol. *121*, pp. 277–288, AGU, Washington, D. C.

Keskin, M. (2003), Magma generation by slab steepening and breakoff beneath a subduction-accretion complex: An alternative model for collision-related volcanism in Eastern Anatolia, Turkey, *Geophys. Res. Lett.*, *30*(24), 8046, doi:10.1029/2003GL018019.

Kincaid, C., and P. Olson (1987), An experimental study of subduction and slab migration, *J. Geophys. Res.*, *92*, 13,832–13,840

Larson, R. L., and C. Kincaid, (1996), Onset of mid-Cretaceous volcanism by elevation of the 670 km thermal boundary layer, *Geology*, *24*, 551–554.

Li, C., R. D. van der Hilst, A. S. Meltzer, and E. R. Engdahl (2008), Subduction of the Indian lithosphere beneath the Tibetan Plateau and Burma, *Earth Planet. Sci. Lett.*, *274*, 157–168.

Lithgow-Bertelloni, C., and M. A. Richards (1998), The dynamics of Cenozoic and Mesozoic plate motions, *Rev. Geophys. 36*, 27–78.

Lithgow-Bertelloni, C., and P. G. Silver (1998), Dynamic topography, plate driving forces and the African superswell, *Nature*, *395*, 269–272.

Liu, L., S. Spasojevic, and M. Gurnis (2008), Reconstructing Farallon plate subduction beneath North America back to the Late Cretaceous, *Science*, *322*, 934–938.

Liu, L., M. Gurnis, M. Seton, J. Saleeby, R. D. Müller, and J. M. Jackson (2010), The role of oceanic plateau subduction in the Laramide orogeny, *Nat. Geosci.*, *3*, 353–357.

Machetel, P., and P. Weber (1991), Intermittent layered convection in a model mantle with an endothermic phase change at 670 km, *Nature*, *350*, 55–57.

McNamara, A. K., and S. Zhong (2005), Thermochemical structures beneath Africa and the Pacific Ocean, *Nature*, *437*, 1136–1139.

Molnar, P., and T. Atwater (1979), Interarc spreading and cordilleran tectonics as alternates related to the age of subducted oceanic lithosphere, *Earth Planet. Sci. Lett.*, *41*, 330–340.

Molnar, P., and P. Tapponnier (1975), Cenozoic tectonics of Asia: Effects of a continental collision, *Science*, *189*, 419–426.

Molnar, P., P. C. England, and J. Martinod (1993), Mantle dynamics, uplift of the Tibetan plateau, and the Indian monsoon, *Rev. Geophys.*, *31*, 357–396.

Moore, A., T. Blenkinsop, and F. Cotterill (2009), Southern African topography and erosion history: Plumes or plate tectonics?, *Terra Nova*, *21*, 310–315.

Moucha, R., and A. Forte (2011), Changes in African topography driven by mantle convection *Nat. Geosci.*, *4*(10), 707–712.

Müller, R. D., M. Sdrolias, C. Gaina, B. Steinberger, and C. Heine (2008), Long-term sea-level fluctuations driven by ocean basin dynamics, *Science*, *319*, 1357–1362.

Najman, Y., and E. Garzanti (2000), Reconstructing early Himalayan evolution and paleogeography from Tertiary foreland basin sedimentary rocks, northern India, *Geol. Soc. Am. Bull.*, *112*, 435–449.

Nataf, H.-C., and Y. Ricard (1996), 3SMAC: An *a priori* tomographic model of the upper mantle based on geophysical modeling, *Phys. Earth Planet. Inter.*, *95*, 101–122.

Ni, S., E. Tan, M. Gurnis, and D. Helmberger, (2002), Sharp sides to the African superplume, *Science*, *296*, 1850–1852.

Oncken, O., D. Hindle, J. Kley, K. Elger, P. Victor, and K. Schemmann (2006), Deformation of the central Andean Upper Plate System: Facts, fiction, and constraints for plateau models, in *The Andes*, vol. 12, *Frontiers in Earth Sciences*, edited by O. Oncken et al., pp. 3–28, Springer, New York.

Partridge, T. C. (1997), Landscape evolution, in *Vegetation of Southern Africa*, edited by R. M. Cowling, D. M. Richardson, and S. M. Pierce, pp. 1–18, Cambridge Univ. Press, Cambridge, U. K.

Partridge, T. C., and R. R. Maud (1987), Geomorphic evolution of southern Africa since the Mesozoic, *S. Afr. J. Geol.*, *90*, 165–184.

Patriat, P., and J. Achache (1984), India–Eurasia collision chronology has implications for crustal shortening and driving mechanism of plates, *Nature*, *311*, 615–621.

Platt, J. P. (1986), Dynamics of orogenic wedges and the uplift of high-pressure metamorphic rocks, *Geol. Soc. Am. Bull.*, *97*, 1037–1053.

Pubellier, M., et al. (2008), *Structural map of eastern Eurasia*, Comm. de la Carte Geol. du Monde, Paris.

Pysklywec, R. N., and M. Ishii (2005), Time dependent subduction dynamics driven by the instability of stagnant slabs in the transition zone, *Phys. Earth Planet. Inter.*, *149*, 115–132.

Pysklywec, R. N., and J. X. Mitrovica (1997), Mantle avalanches and the dynamic topography of continents, *Earth Planet. Sci. Lett.*, *148*, 447–455.

Pysklywec, R. N., J. X. Mitrovica, and M. Ishii (2003), Mantle avalanche as a driving force for tectonic reorganization in the southwest Pacific, *Earth Planet. Sci. Lett.*, *209*, 29–38.

Qin, Y., Y. Capdeville, J.-P. Montagner, L. Boschi, and T. W. Becker (2009), Reliability of mantle tomography models assessed by spectral-element simulation, *Geophys. J. Int.*, *177*, 125–144.

Ren, Y., E. Stutzmann, R. D. Van der Hilst, and J. Besse, (2007), Understanding seismic heterogeneities in the lower mantle beneath the Americas from seismic tomography and plate tectonic history, *J. Geophys. Res.*, *112*, B01302, doi:10.1029/2005JB004154.

Replumaz, A., H. Kárason, R. D. van der Hilst, J. Besse, and P. Tapponnier (2004), 4-D evolution of SE Asia's mantle from geological reconstructions and seismic tomography, *Earth Planet. Sci. Lett.*, *221*, 103–115.

Replumaz, A., A. Negredo, S. Guillot, and A. Villaseñor (2010), Multiple episodes of continental subduction during India/Asia convergence: insight from seismic tomography and tectonic reconstruction, *Tectonophysics*, *483*, 125–134.

Ricard, Y., and C. Vigny (1989), Mantle dynamics with induced plate tectonics, *J. Geophys. Res.*, *94*, 17,543–17,559.

Ricard, Y., M. A. Richards, C. Lithgow-Bertelloni, and Y. LeStunff (1993), Geodynamic model of mantle density heterogeneity, *J. Geophys. Res. 98*, 21,895–21,909.

Ritsema, H. J., J. H. van Heijst, and J. H. Woodhouse (1999), Complex shear velocity structure beneath Africa and Iceland, *Science*, *286*, 1925–1928.

Roberts, G. G., and N. White (2010), Estimating uplift rate histories from river profiles using African examples, *J. Geophys. Res.*, *115*, B02406, doi:10.1029/2009JB006692.

Romanowicz, B., and Y. Gung (2002), Superplumes from the core–mantle boundary to the lithosphere: implications for heat flux, *Science*, *296*, 513–516.

Rowley, D. B. (1996), Age of initiation of collision between India and Asia: A review of stratigraphic data, *Earth Planet. Sci. Lett.*, *145*, 1–13.

Royden, L. H. (1993a), The tectonic expression slab pull at continental convergent boundaries, *Tectonics*, *12*, 303–325, doi:10.1029/92TC02248.

Royden, L. H. (1993b), Evolution of retreating subduction boundaries formed during continental collision, *Tectonics*, *12*, 629–638, doi:10.1029/92TC02641.

Royden, L., E. Patacca, and P. Scandone (1987), Segmentation and configuration of subducted lithosphere in Italy: An important control on thrust-belt and foredeep-basin evolution, *Geology*, *15*, 714–717.

Russo, R. M., and P.G. Silver (1996), Cordillera formation, mantle dynamics, and the Wilson cycle, *Geology*, *24*, 511–514.

Schellart, W. P., J. Freeman, D. R. Stegman, and L. Moresi (2007), Evolution and diversity of subduction zones controlled by slab width, *Nature*, *446*, 308–311.

Schubert, G., D. L. Turcotte, and P. Olson (2001), *Mantle Convection in the Earth and Planets*, Cambridge Univ. Press, Cambridge, U. K.

Sdrolias, M., and R. D. Müller (2006), Controls on back-arc basin formation, *Geochem. Geophys. Geosyst.*, *7*, Q04016, doi:10.1029/2005GC001090.

Silver, P., R. M. Russo, and C. Lithgow-Bertelloni (1998), Coupling of South American and African plate motion and plate deformation, *Science*, *279*, 60–63.

Solheim, L. P., and W. R. Peltier (1994), Avalanche effects in phase transition modulated thermal convection: A model of Earth's mantle, *J. Geophys. Res.*, *99*, 6997–7018.

Stampfli, G. M., and G. D. Borel (2002), A plate tectonic model for the Paleozoic and Mesozoic constrained by dynamic plate boundaries and restored synthetic oceanic isochrons, *Earth Planet. Sci. Lett.*, *196*, 17–33.

Steinberger, B. (2000), Slabs in the lower mantle—Results of dynamic modeling compared with tomographic images and the geoid, *Phys. Earth Planet. Inter.*, *118*, 241–257.

Steinberger, B., and A. Calderwood (2006), Models of large-scale viscous flow in the Earth's mantle with constraints from mineral physics and surface observations, *Geophys. J. Int.*, *167*, 1461–1481.

Su, W., and A. M. Dziewonski (1997), Simultaneous inversion for 3-D variations in shear and bulk velocity in the mantle, *Phys. Earth Planet. Inter.*, *100*, 135–156.

Tackley, P. J., D. J. Stevenson, G. A. Glatzmaier, and G. Schubert (1993), Effects of an endothermic phase transition at 670 km depth in a spherical model of convection in the Earth's mantle, *Nature*, *361*, 699–704.

Torsvik, T. H., R. D. Tucker, L. D. Ashwal, L. M. Carter, B. Jamtveit, K. T. Vidyadharan, and P. Venkataramana (2000), Late Cretaceous India-Madagascar fit and timing of break-up related magmatism, *Terra Nova*, *13*, 220–224.

Torsvik, T., R. Muller, R. van der Voo, B. Steinberger, and C. Gaina (2008), Global plate motion frames: Toward a unified model, *Rev. Geophys.*, *46*, RG3004, doi:10.1029/2007RG000227.

Torsvik, T. H., B. Steinberger, M. Gurnis, and C. Gaina (2010), Plate tectonics and net lithosphere rotation over the past 150 My, *Earth Planet. Sci. Lett.*, *291*, 106–112.

van der Hilst, R. D., and T. Seno (1993), Effects of relative plate motion on the deep structure and penetration depth of slabs below the Izu–Bonin and Mariana island arcs, *Earth Planet. Sci. Lett.*, *120*, 375–407.

van der Hilst, R. D., S. Widiyantoro, and E. R. Engdahl (1997), Evidence for deep mantle circulation from global tomography, *Nature*, *386*, 578–584.

van der Meer, D. G., W. Spakman, D. J. J. van Hinsbergen, M. L. Amaru, and T. H. Torsvik (2010), Toward absolute plate motions constrained by lower mantle slab remnants, *Nat. Geosci.*, *3*, 36–40.

van der Voo, R., W. Spakman, and H. Bijwaard, (1999), Tethyan subducted slabs under India, *Earth Planet. Sci. Lett.*, *171*, 7–20.

van Hinsbergen, D. J. J., E. Hafkenscheid, W. Spakman, J. E. Meulenkamp, and M. J. R. Wortel (2005), Nappe stacking resulting from subduction of oceanic and continental lithosphere below Greece, *Geology*, *33*, 325–328.

van Hinsbergen, D. J. J., P. Kapp, G. Dupont-Nivet, P. Lippert, P. DeCelles, and T. Torsvik (2011a), Restoration of Cenozoic deformation in Asia, and the size of Greater India, *Tectonics*, *30*, TC5003, doi:10.1029/2011TC002908.

van Hinsbergen, D. J. J., B. Steinberger, P. Doubrovine, and R. Gassmöller (2011b), Acceleration-deceleration cycles of India-Asia convergence: Roles of mantle plumes and continental collision, *J. Geophys. Res.*, *116*, B06101, doi:10.1029/2010JB008051.

van Hinsbergen, D. J. J., P. C. Lippert, G. Dupont-Nivet, N. McQuarrie, P. V. Doubrovine, W. Spakman, and T. H. Torsvik (2012), Greater India Basin hypothesis and a two-stage Cenozoic collision between India and Asia, *Proc. Natl. Acad. Sci. U. S. A.*, *109*, 7659–7664.

van Summeren, J., C. P. Conrad, and C. Lithgow-Bertelloni (2012), The importance of slab pull and a global asthenosphere to plate motions, *Geochem. Geophys. Geosyst.*, *13*, Q0AK03, doi:10.1029/2011GC003873.

Wilson (1961), Continent and oceanic differenziation, *Nature*, *192*, 125–128.

Wu, B., C. P. Conrad, A. Heuret, C. Lithgow-Bertelloni, and S. Lallemand (2008), Reconciling strong slab pull and weak plate bending: The plate motion constraint on mantle slabs, *Earth Planet. Sci. Lett.*, *272*, 412–421.

Zandt, G., S. L. Beck, S. R. Ruppert, C. J. Ammon, D. Rock, E. Minaya, T. C. Wallace, and P. G. Silver (1996), Anomalous crust of the Bolivian Altiplano, central Andes: Constraints from broadband regional seismic waveforms, *Geophys. Res. Lett.*, *23*, 1159–1162.

Zhang, Z.-K., M. Wang, W. Gan, R. Burgmann, Q. Wang, Z. Niu, J. Sun, J. Wu, S. Hanrong, and Y. Xinzhao (2004), Continuous deformation of the Tibetan Plateau from global positioning system data, *Geology*, *32*, 809–812.

Zhong, S., and M. Gurnis (1995), Mantle convection with plates and mobile, faulted plate margins, *Science*, *267*, 838–842.

Zhong, S., M. T. Zuber, L. Moresi, and M. Gurnis (2000), Role of temperature-dependent viscosity and surface plates in spherical shell models of mantle convection, *J. Geophys. Res.*, *105*, 11,063–11,082.